



TIME-DOMAIN BEAMFORMING TO CHARACTERIZE INTERMITTENT NOISE SOURCES IN A MINING MILL

Jeffrey Fischer¹, Wei Chen² and Con Doolan²

¹ School of Mechanical and Manufacturing Engineering, UNSW Sydney
High street, NSW 2052, Sydney, Australia

² Bradken

20 McIntosh Drive Mayfield West, NSW 2304, Newcastle, Australia

Abstract

The University of New South Wales (UNSW) has collaborated with Bradken and with the University of Queensland (UQ) to conduct some acoustic testing on a scaled mining mill. The mill, located at the Julius Kruttschnitt Mineral Research Centre (JKMRC), has a diameter of 1.8 m and was filled with water, rocks and iron balls. The amount of balls as well as the rotating speed of the mill were varied: the mass of balls was respectively set to 0%, 5%, 10% and 15% of the total mass while the rotating speed was successively set to 50%, 60%, 70%, 80% and 90% of the mill maximal rotating speed, which is about 30 rotations per minute. An acoustic array of 2 m diameter and composed of 64 microphones was placed in front of the mill. The data were processed using beamforming in the frequency and time domains. A threshold was used in order to select intermittent events in the signals. The acoustic maps show the location of the sound sources at different instants, mostly located at the centre of the mill; some statistics on the sources intermittency are also proposed.

1 INTRODUCTION

Introduction

Grinding mills are used to reduce the size of ore materials, so that they can be used for mineral enrichment processing. For that purpose, the grinding mills are usually filled with rocks, water and steel balls. These elements directly influence the dynamic charge behaviour within the mill, which is the key metric for operational diagnostics. In order to optimize the mill efficiency, it is important to understand the effect of the different parameters (charges within the mill and rotational speed) on the crushing process.

Several tools have been developed for that purpose. Some wireless mill charge detection methods have been developed, by embedding strain gauges and integrated circuitry with grinding steel balls [7]. The movements of the mill charge can then be recorded both in the rotating and the longitude direction of the mill. However, transmitting data out of the steel mill shell wirelessly is quite difficult; also the on-board measurement data can be damaged due to the subsequent degradation of the steel balls during mill operation.

Another option is to have the measuring devices either installed on the mill shell or embedded in liners [8, 14, 15]. Some examples of the commonly used devices are the electrical conductivity probes, the piezoelectric strain transducers [6] and the accelerometers. The latter measures the mechanical vibration of the mill during operation and uses it to determine the approximate positions of the charge shoulder and toe. However, this approach still requires modification/addition to the mill shell/liners, and it can potentially threaten the safe operation of the grinding mill once installed onto a large area of the mill shell.

In terms of numerical approaches, discrete element modelling (DEM) has been used to understand the behaviour of the dynamic charge inside the mill [2, 3]. An example is shown in Fig. 1 and shows that most of the charge is found in an area that is similar to a "kidney bean" shape. Nevertheless, it is essential to validate the numerical modelling results experimental measurements to ensure the accurate representation of the reality.

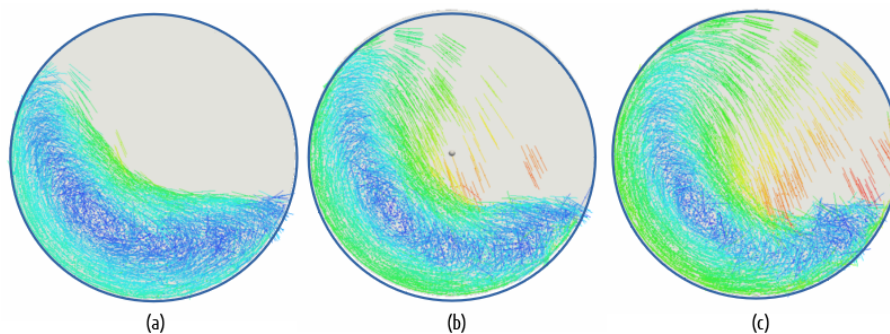


Figure 1: Different modes of dynamic charge behaviours in a rotating mill in three different regimes: (a) under throw grinding of the mill charge; (b) correct throw of the mill charge; (c) over throw of the mill charge.

Thus, it is preferable to use non-invasive measurement techniques as they provide safer, yet effective on-line charge monitoring solutions. Beamforming is a very popular acoustic tool to identify noise sources in various environments [1, 9, 13]. It can be used on grinding mills to detect and reconstruct the differentiated sound characteristics generated during ball, rock and liner contacts. Therefore, the aim of the present study is to characterize the intermittency of the noise sources inside the rotating mill. The latter is filled with rocks, steel balls and water. The conventional beamforming algorithm used to plot acoustic maps is modified in order to investigate intermittent noise sources [4, 5, 12]. In addition, some intermittent event detection is performed using single microphone measurements in order to analyse the effect of different parameters on the occurrence of peaks in the signal.

2 EXPERIMENTAL SET UP

2.1 Mill

The mill dimensions are presented in Fig. 2. Its diameter is 1.8 m and it sits inside a wooden enclosure. This enclosure was designed specifically for this project, so that the acoustic array could fit inside. A photograph of the set up is shown in Fig. 3(a), with the mill (background), the acoustic array (mounted on the aluminium structure), and the enclosure.

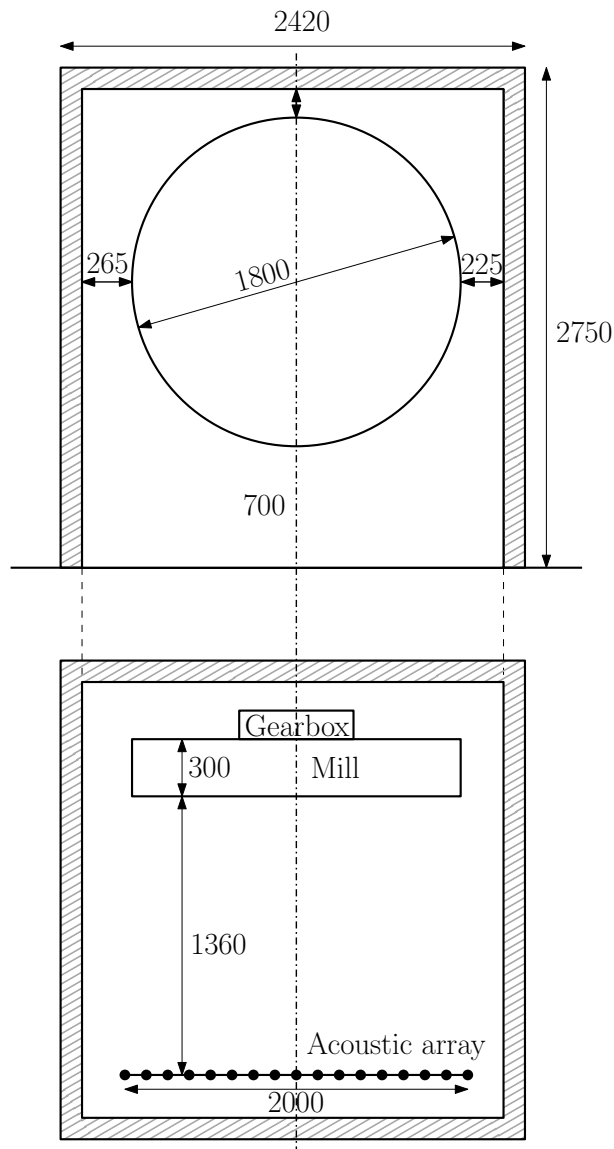


Figure 2: Dimension of the mill and enclosure: Front view (top) and top view (bottom).

2.2 Microphone acoustic array

Acoustic measurements have been conducted using a microphone array located in front of the mill, at 1.36 m from it (see Fig. 2). The array is composed of 64 1/4" GRAS 40PH phase matched microphones (frequency range [50 Hz ; 10 kHz]). Those microphones are mounted on a 2 m × 2 m perforated steel grid using plastic cable glands. The array has an optimal design for beamforming applications [11] and is scaled for the purpose of this particular study; it consists of 7 concentric circles of 9 microphones each, as shown in Fig. 3(b). The array centre microphone is centered with the mill centre of rotation. Due to technical difficulties, only the x axis is aligned properly. In the y direction, the array centre is located 7 cm below the mill centre.

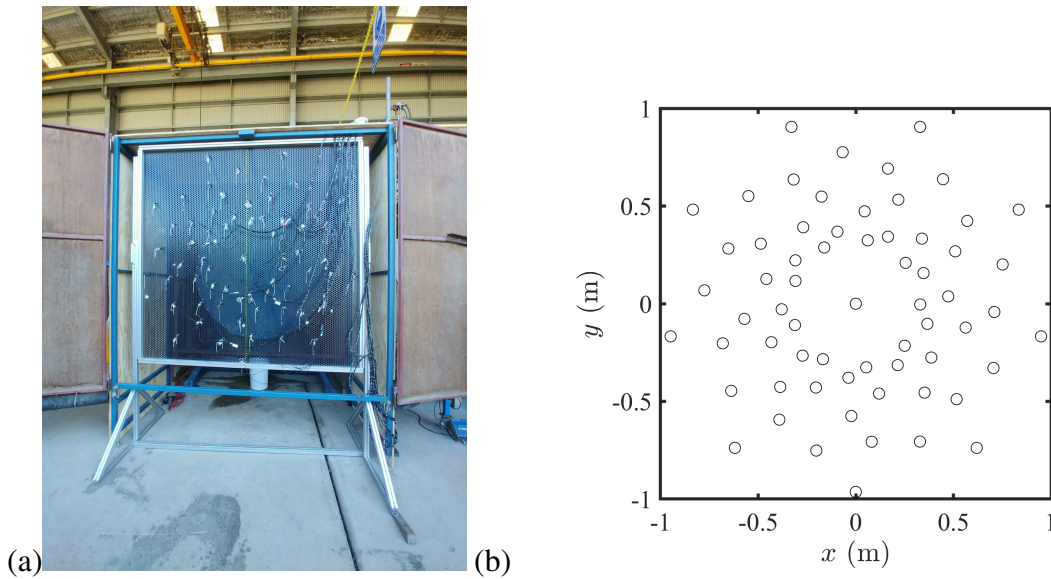


Figure 3: (a) Photograph of the experimental set up and (b) sketch of the acoustic array geometry.

2.3 Processing parameters

The array microphones are connected to a PXIe-4499 24-bit simultaneous sample computer. The signals are acquired during $T = 32$ s at a sampling frequency $f_s = 65,536$ Hz. The acoustic spectra are obtained using Welch's periodogram [10] with the following input parameters: $N_{FFT} = 8192$ pts, $N_{overlap} = N_{FFT}/2$ and a Hann window. The spectra and acoustic maps are presented in decibel (dB) using the reference acoustic pressure in air $p_0 = 20 \mu\text{Pa}$.

2.4 Test conditions

The mill is filled with different amounts of steel balls, rocks and water. The water and rock mass are kept constant respectively at 86 kg and 259 kg for all the tests; this corresponds to a rock proportion of 15% of the total volume inside the mill. Only two parameters are varied in this study: the mill rotational speed and the ball filling. The rotational speed is set to 50%, 60%,

70%, 80% and 90% of the mill's critical speed (about 30 RPM). The ball filling is respectively set to 0%, 5%, 10% and 13.3% of the mill volume. All the cases are summarized in Table 1. Also, the characteristics of the steel balls for each case can be found in Table 2.

Test No	Speed % critical	Balls filling %	Rocks filling %	Total Filling %
01	50	0	15	15
02	50	5	15	20
03	50	10	15	25
04	50	13.3	15	28.3
05	60	0	15	15
06	60	5	15	20
07	60	10	15	25
08	60	13.3	15	28.3
09	70	0	15	15
10	70	5	15	20
11	70	10	15	25
12	70	13.3	15	28.3
13	80	0	15	15
14	80	5	15	20
15	80	10	15	25
16	80	13.3	15	28.3
17	90	0	15	15
18	90	5	15	20
19	90	10	15	25
20	90	13.3	15	28.3

Table 1: Summary of all the cases.

Balls filling %	Balls volume L	Balls mass kg
0	0	0
5	37.6	293.4
10	75.1	586.9
13.3	112.7	782

Table 2: Iron balls characteristics.

3 BEAMFORMING ANALYSIS

3.1 Spectra

The acoustic spectra for the array centre microphone are displayed in Fig. 4, respectively for fixed speeds and fixed ball fillings. First, the mill speed was set to 50% (Fig. 4(a)) and 90% (Fig. 4(b)) of its critical speed, and the ball fillings were varied from 5% to 15% with 5% increments. When the ball filling is changed from 5% to 10%, the acoustic spectra increase by about 3 to 5 dB depending on the mill speed. Finally, no difference is observed between the 10% and 15% filling cases in terms of noise.

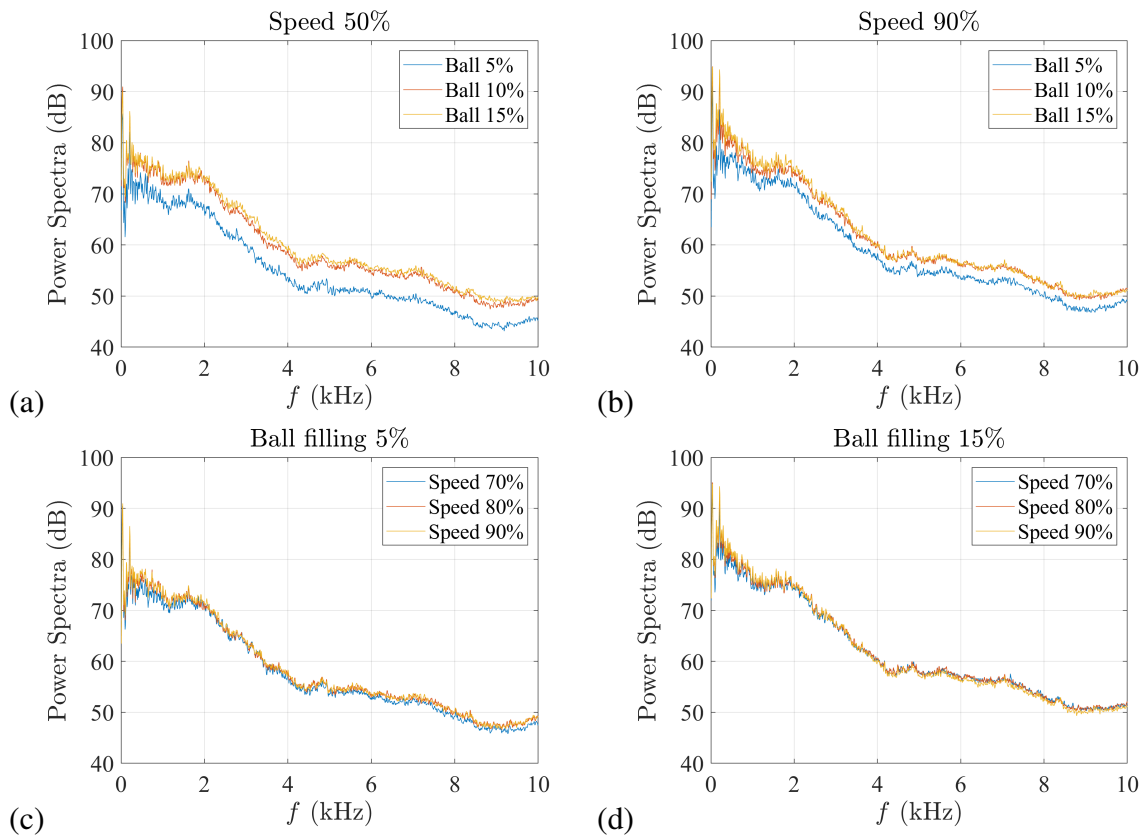


Figure 4: Spectra of the array centre microphone for various configurations: a rotational speed of (a) 50% and (b) 90% of critical speed, and a ball filling of (c) 5% and (d) 15% of the mill volume.

The influence of the mill speed is shown in Fig. 4(c) and (d). For a ball filling of 5% (Fig. 4(c)), the increase of speed results in a slight increase of radiated noise, of about 1 dB per speed. However, when the amount of balls is more important (Fig. 4(d)), the spectra all look similar.

These results have shown that the amount of ball filling has a great impact on the radiated noise, especially at low speeds. However, the change in the mill speed has little impact on the acoustic radiation.

3.2 Conventional Beamforming (CBF)

Some acoustic maps are presented in Fig. 5. The circle denotes the mill circumference, and each dot represents a microphone location. The values in the colormap correspond to the acoustic noise level and are given in decibel (dB). Each figure corresponds to a different 1/3rd octave band, ranging from 500 Hz to 1600 Hz. These maps correspond to the highest balls filling (15%) and the highest mill speed (90%). At $f = 500$ Hz, the shape in the mill area looks similar to the simulation results (kidney bean shape). But the higher level of the surrounding lobes make it difficult to observe due to the dynamic range. At 630 Hz, a source is found in the centre of the mill, and some surrounding lobes are also present all around the mill circumference. Up to 1 kHz, the source in the centre is still observed, but at higher frequencies the map is similar to a background noise result.

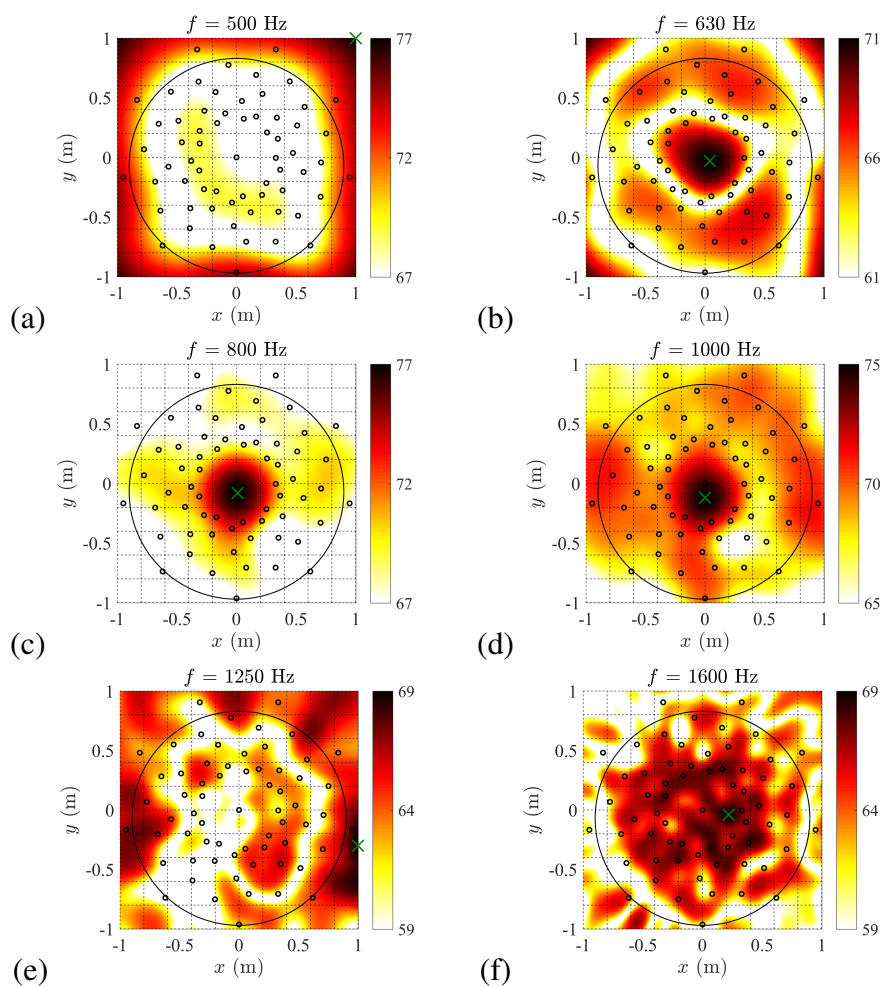


Figure 5: CBF maps obtained with the highest ball filling (15%) and the highest mill speed (90%) for several 1/3rd octave bands between 500 Hz and 1600 Hz.

In order to focus at the kidney bean shape found at 500 Hz, the CBF maps for all the tests cases are shown at this particular frequency in Fig. 6. In order to increase the level of that source, the outer sources located outside of the mill area have been removed. Each column

corresponds to a different amount of iron balls, and each row stands for a different mill speed. When no balls are present, the kidney bean shape is not found. It only appears for 5% to 15% filling, and has a different shape depending on the case. It appears that the change in ball filling has a greater impact on the shape than the change in speed.

It must be noted that all the results shown until now were obtained using the full time serie of the measurement (32 s). However, the experiments have shown that the sound is quite intermittent, with several impact noise that occur randomly during each set. These random impacts are investigated in the next section.

3.3 Short-Time Beamforming (ST-BF)

Figure 7 shows a sample of a time serie obtained with one microphone during one of the tests. It appears that the signal contains some higher amplitude events that most certainly correspond to ball impacts in the mill. In order to investigate them, the signal is cut into two parts: one segment before the impact (green box) and one after the impact (red box). The corresponding beamforming maps, known as Short-Time Beamforming (ST-BF), are displayed in Fig. 8, respectively in the left and right column. Before the impact, the noise location is not clearly found, except at 800 Hz where it seems located in the mill centre. However, after the impact, a dominant noise source is present in the mill centre from 630 Hz to 1 kHz, which is similar to the conclusions from the previous section.

3.4 Time-Domain Beamforming (TD-BF)

In order to investigate individual peaks in the microphone signals, the beamforming algorithm is computed in its time-domain version; this is known as Time-Domain Beamforming (TD-BF). Thus, an acoustic map is obtained at each time step. At each time step, the spatial maximum is found and its amplitude is saved. This process is very long; it takes around 8 h to process 10,000 time steps. Thus, the results shown in this section were obtained with that number of samples (and corresponds to a signal length of 0.15 s). In Fig. 9, the maximal amplitude in each map is shown versus the time steps. In other words, that figure shows the time evolution of the maximum level on the sound map. Note that the acoustic maps were filtered in the 1/3rd octave band 500 Hz as it was observed in the CBF results that the expected "kidney bean" shape was found at this frequency.

It can be observed that the function in Fig. 9 looks like a succession of step functions: the function increases, reaches a peak and then drops. Each of these local peaks correspond to the presence of an acoustic source. If we are to investigate the highest peaks, a threshold β can be used, as shown in Fig. 9 with the red dashed lines ($\beta = 0.5$). In that case, only the peaks higher than this threshold are located (denoted by the red circles). How this threshold is chosen is still an undergoing study.

Once the peaks are chosen, it is possible to observe the acoustic maps surrounding those peaks. An example of this is shown in Fig. 10 where 5 different maps are displayed around a peak located at t_0 . As can be seen, before the maximum is found, some converging wave fronts appear on the maps (Fig. 10(a) to (d)). After the maximum at t_0 , those wave fronts disappear (Fig. 10(e) and (f)). These converging wave fronts are the reason for the increase in the step-like functions from Fig. 9. These results are similar to what was observed by [4, 5, 12].

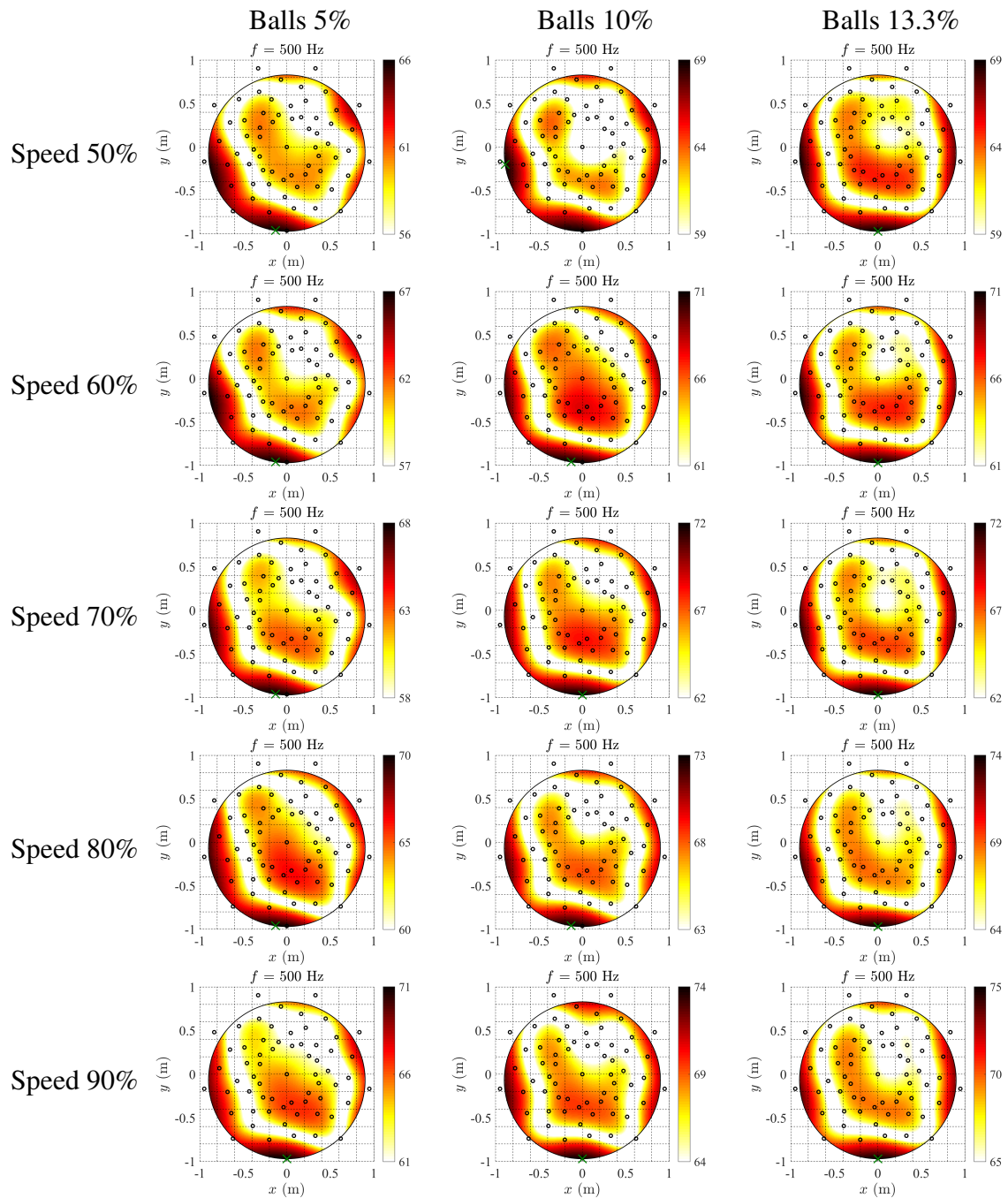


Figure 6: CBF maps in the 1/3 octave band 500 Hz for all the cases: ball fillings are in columns (5%, 10% and 15%) and mill speeds are in rows (50%, 60%, 70%, 80% and 90%). The region outside of the mill was removed.

Once all the peaks are detected over the 10,000 time steps, their location can be plotted on the mill. Figure 11 shows those peak locations for 4 different configurations: the ball filling is respectively (a) 0 %, (b) 5 %, (c) 10 % and (d) 15%; the mill speed is set to 90% of its

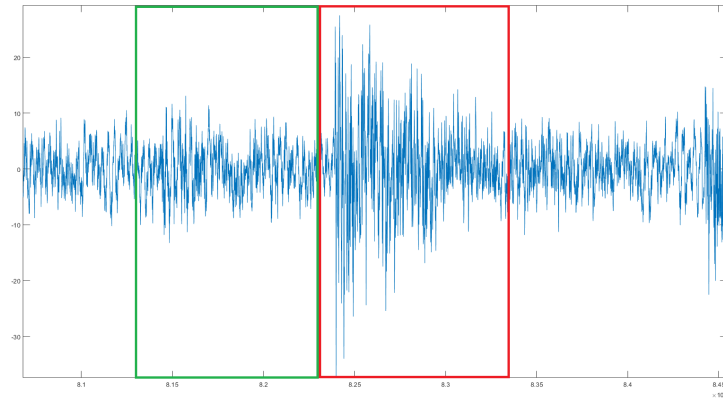


Figure 7: Example of two time blocks before (green) and after (red) an impact during the test.

critical speed. It appears that in all the cases, most of the noise sources are located around the centre of the mill. Some peaks are found outside of the mill and could be due to reflections in the confined reverberant environment. Also, no major difference is observed between each configuration, which leads to the conclusion that the concentration of steel balls does not affect the sound location over this short period of time (0.15 s) in the 500 Hz 1/3rd octave band.

4 STATISTICAL ANALYSIS OF THE TIME SERIES FOR IMPACT NOISE DETECTION

In the previous section, the data were analysed using beamforming methods which is an efficient tool for localizing sound sources but requires many sensors. However, impact noise can also be detected in single microphone measurements but require different processing methods. The current section is dedicated to the detection and analysis of impacts using one microphone (the array centre microphone). Note that all the statistics in this section are obtained using the whole length of the signal of $T = 32$ s.

4.1 Peak detection

The detection of intermittency in acoustic signals is usually performed by first defining a threshold on the pressure signal; any part of the signal below that threshold will not be considered for the intermittency detection. That threshold β can be defined as a function of the standard deviation of the pressure signal σ_p . In other words, the signal of interest is $p(t)/\sigma_p$. For any given time segment Δt_i , two cases can occur:

- if $\frac{|p(\Delta t_i)|}{\sigma_p} < \beta$, no peak is sought.
- if $\frac{|p(\Delta t_i)|}{\sigma_p} \geq \beta$, a peak search is conducted.

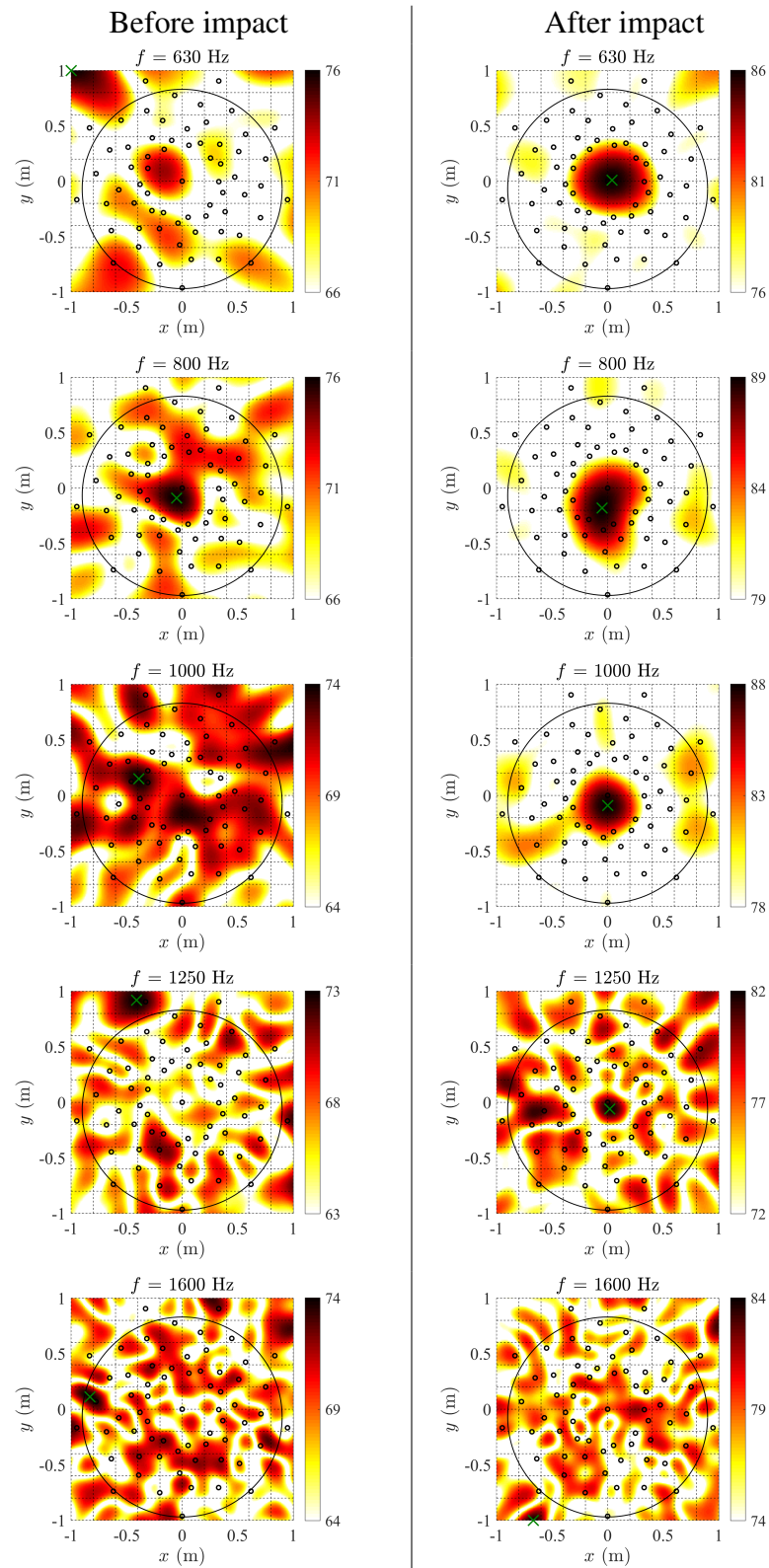


Figure 8: Example of beamforming maps before (left) and after (right) an impact during the test. Results are shown for several 1/3rd octave bands from 630 Hz to 1.6 kHz.

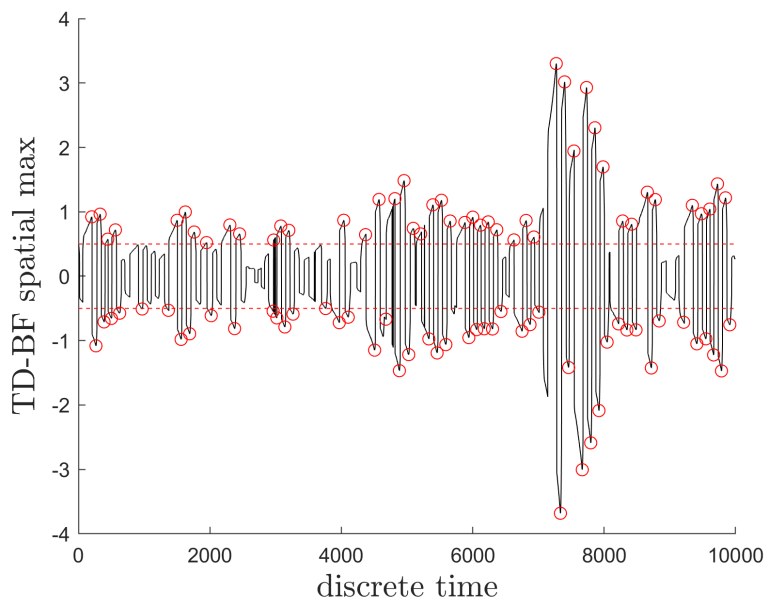


Figure 9: Evolution of the maximum on the TDB-BF maps over 10,000 time steps. The red dashed line denotes the threshold for the peak detection (red circles). Ball filling 15% and mill rotational speed 90%.

An example is given in Fig. 12, where the blue plot shows a time series sample obtained with the raw data (no filtering). It can be seen that the signal contains some clear peaks, but also some maxima with a smaller prominence. In order to remove some of these smaller maxima, the signal can be filtered with a Low-Pass (LP) filter. The CBF results from the previous section have shown that the sound sources in the mill are detected at frequencies below 1kHz. Thus, all of the results presented in this section are filtered with a LP filter at 1kHz. An example is shown in Fig. 12 where the red plot corresponds to the same signal as the blue plot but using a LP filter at 1kHz.

Once the filtered signal is obtained, and a threshold is defined, the peaks can be sought. Those are represented by the orange circles in Fig. 12 for an arbitrary threshold $\beta = 2$ denoted by the black dashed lines.

4.2 Statistical study

The main question when investigating intermittenencies in a signal is how to define the threshold β . A good start is to plot the evolution of the number of detected peaks as a function of that threshold β . Figure 13 shows those plots for several cases. In Fig. 13(a), the mill rotational speed is set to 90% of its critical value and different concentrations of steel ball are compared. In Fig. 13(b), the amount of steel balls is set to 15% and the mill rotational speed is varied from 50% to 90% of its critical speed. Note that the number of peaks on the y axis is normalized by the signal length (in sec), thus providing a result as a frequency (Hz).

Apart from the case where no balls are present (blue plot in Fig. 13(a)), all of the curves are very similar. Some slight differences can be observed for small values of β . In Fig. 13(a), the

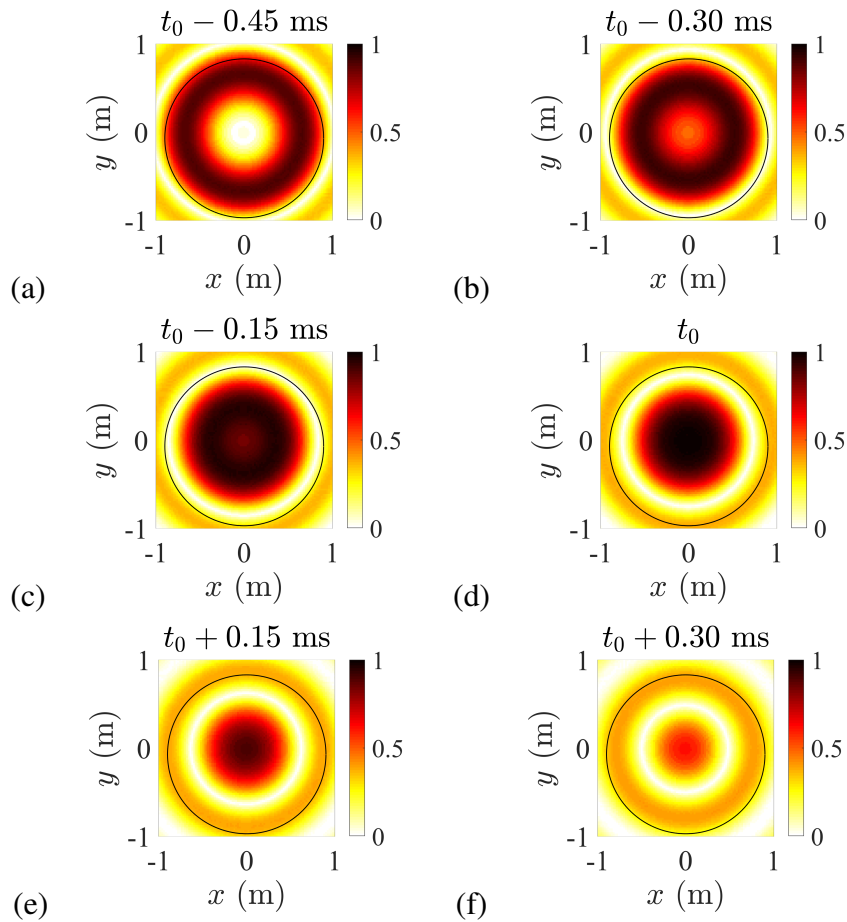


Figure 10: Example of TD-BF maps surrounding a peak (located at t_0 in the time domain). Results are shown in the 1/3 octave band 500 Hz. Ball filling 15% and mill rotational speed 90%.

number of peaks is reduced when the amount of balls is increased. Fig. 13(b), the number of peaks is reduced when the rotational speed is increased. Note that these conclusions are only verified for the small values of β .

Another way to analyse these data is to compare the evolution of the number of peaks as a function of either the ball concentration or the mill rotational speed. These are shown respectively in Fig. 14(a) and (b) for several values of β ranging from 0 to 2 with 0.4 increments. Again, the trends of each curve do not change much between each threshold choice. However, it seems that on both figures (except for the 0% balls case), the number of peaks slightly decreases for $\beta < 0.8$ and slightly increases for $\beta > 0.8$. The case $\beta = 0.8$ shows a constant amount of peaks over the range of ball concentration or mill speed.

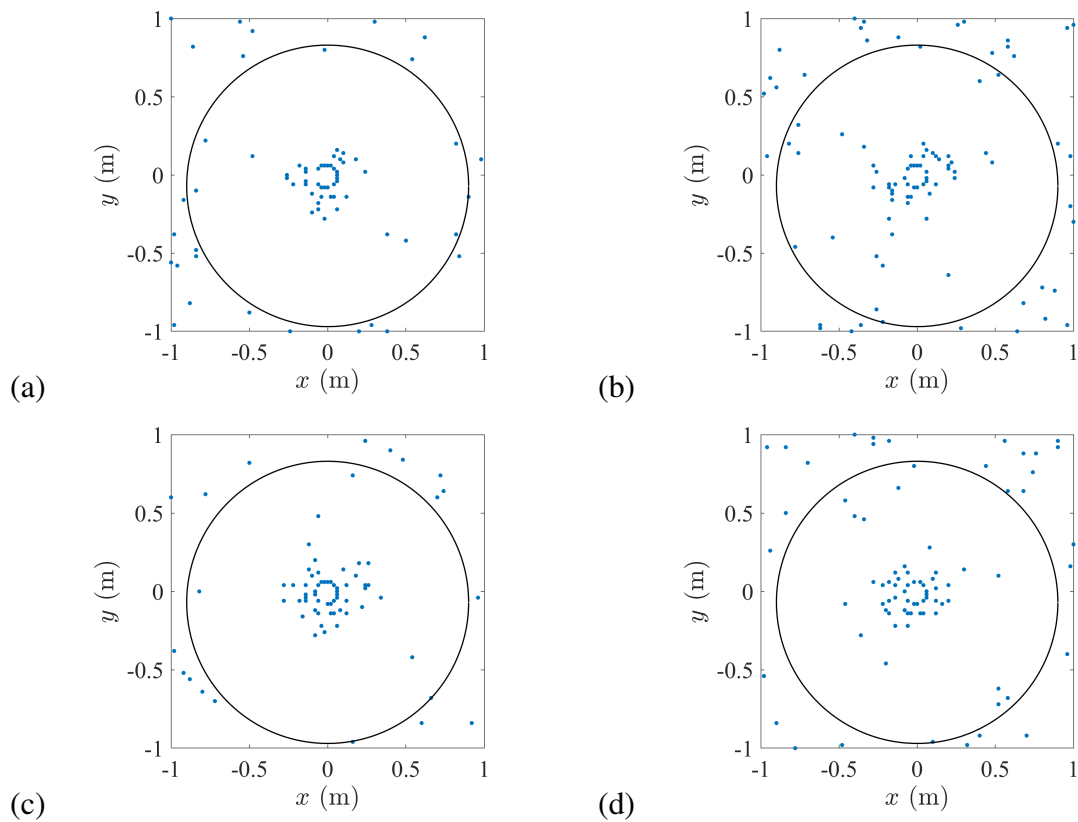


Figure 11: Example of peak locations in the TD-BF map in the 1/3 octave band 500 Hz with the mill running at 90% of its maximal speed and a ball filling of (a) 0 %, (b) 5 %, (c) 10 % and (d) 15%.

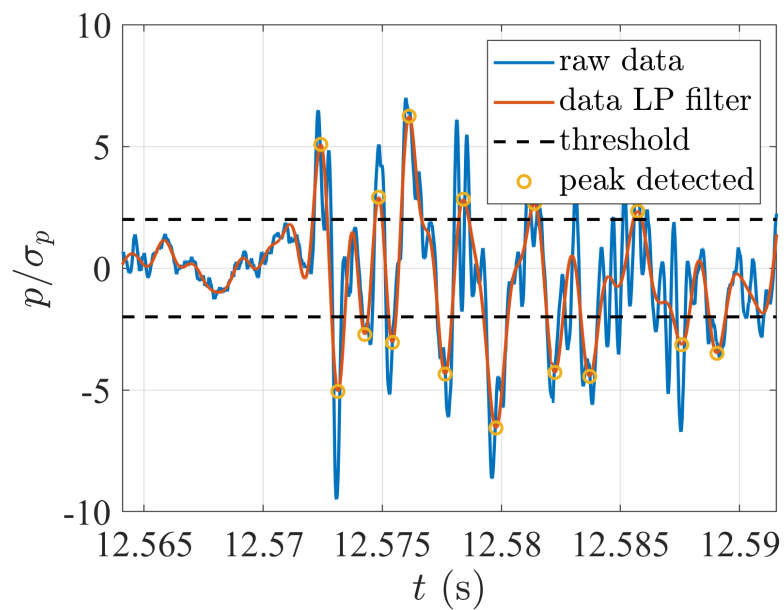


Figure 12: Example of peak locations on a sample of microphone signal. The raw data (blue) and low pass data (red) are superimposed. The threshold $\beta = 2$ is shown in black dashed lines and the resulting peak locations above the threshold are represented by the orange circles. Ball filling 15% and mill rotational speed 90%.

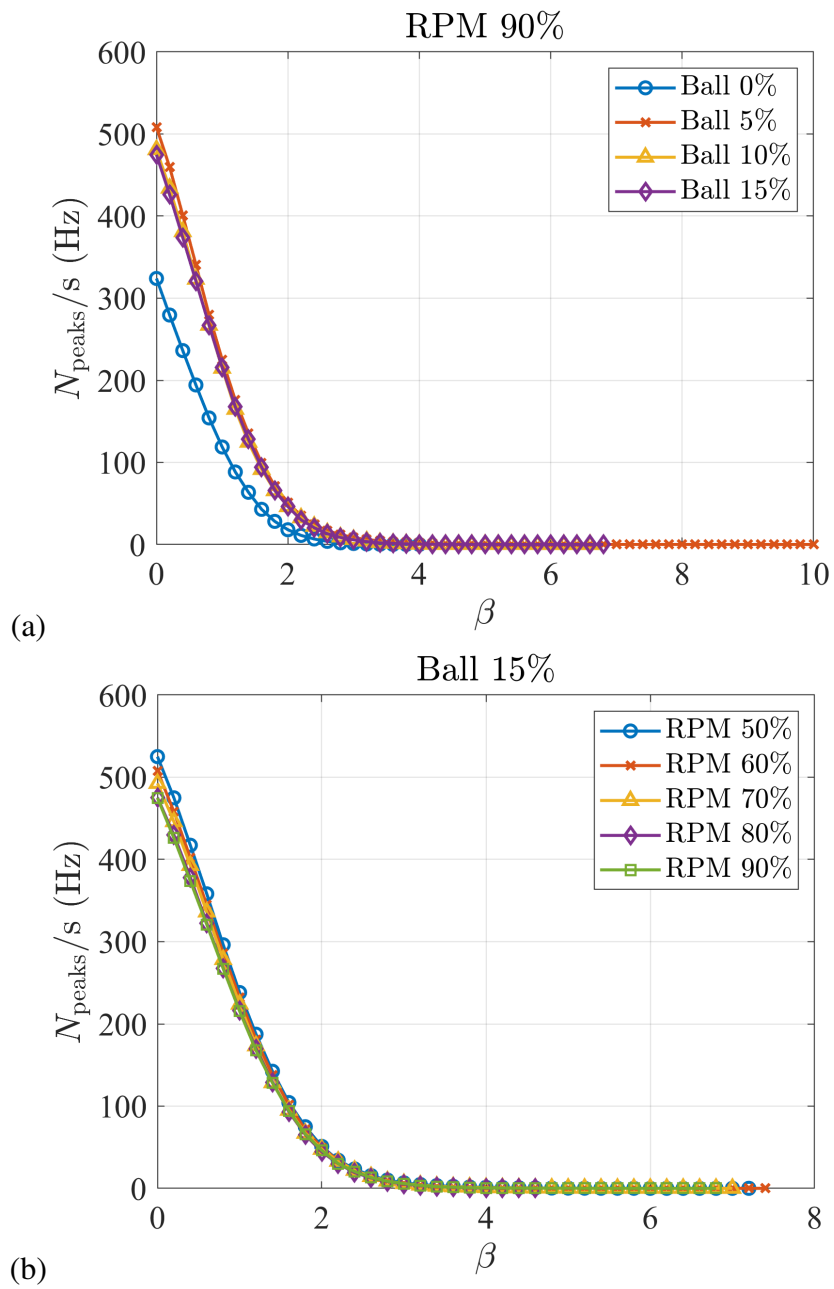


Figure 13: Evolution of the number of detected peaks per second as a function of the threshold β for various configurations. (a) The mill speed is set to 90% and (b) the ball concentration is set to 15%.

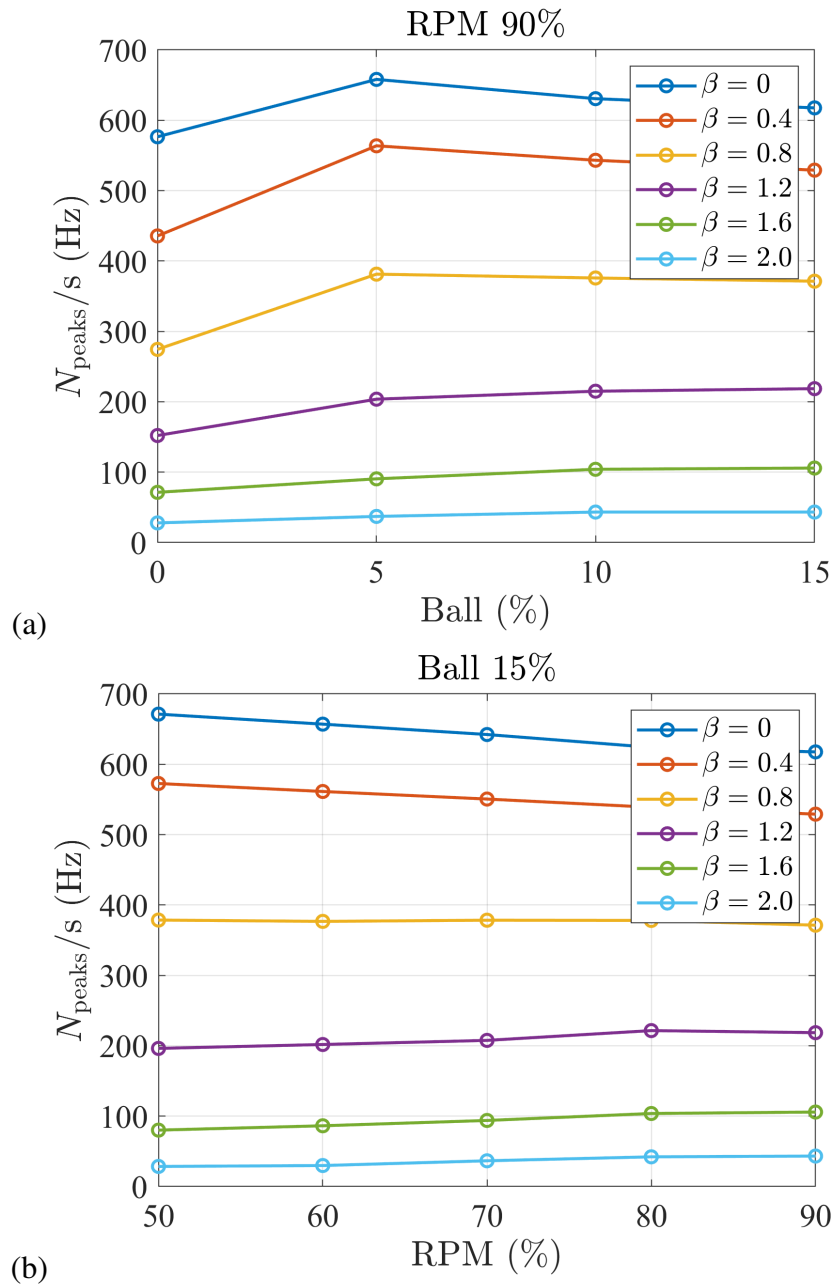


Figure 14: Evolution of the number of detected peaks per second as a function of (a) the ball concentration and (b) the mill speed, for several values of threshold β .

5 CONCLUSION

A thorough analysis of mill sound recordings at JKMRC was presented here. The mill was run for several rotational speeds and steel ball concentrations. The acoustic measurements were obtained using a 64 channels acoustic array of 2 m diameter.

At first, single microphone spectra were compared and led to the conclusion that the steel ball filling has a bigger influence on the radiated noise than the rotational speed. Indeed, the difference between 5% and 10% filling is about 5 dB overall while increasing the speed from 50% to 60% only leads to an increase of 2 dB.

The CBF maps were then analysed. It appeared that the sound sources are only found below 1 kHz. In particular, in the 1/3rd octave band 500 Hz, a "kidney bean" shape is observed. Also, when comparing the acoustic maps before and after an impact, using ST-BF, it appeared that the maps are much cleaner after the impact.

The beamforming algorithm was then modified to its time-domain equivalent (TD-BF) in order to search for intermittent sources. Due to the large processing time, only 10,000 time steps (equivalent to 0.15 s of signal) could be analysed. It appeared that most of the noise sources were located close to the mill centre in the 500 Hz 1/3rd octave band.

Finally, a method was proposed to examine intermittent events in a single microphone signal. At first, the signal is filtered using a low pass filter in order to remove the small high frequency disturbances. Then, some statistics of the peak population are presented for several choices of threshold β . The method can successfully measure the ball impact statistics and the next phase of the work should be to relate these data to real size mill operation.

6 ACKNOWLEDGEMENTS

The authors want to acknowledge Mohsen Yahyaei, Karina Jorge Barbosa and Jiawei Tan for the technical support during the experiments at JKMRC.

7 REFERENCES

REFERENCES

- [1] C. J. Bahr, W. M. Humphreys, D. Ernst, T. Ahlefelds, C. Spehr, A. Pereira, Q. Leclère, C. Picard, R. Porteous, D. J. Moreau, J. Fischer, and C. J. Doolan. "A comparison of microphone phased array methods applied to the study of airframe noise in wind tunnel testing." In *23rd AIAA/CEAS Aeroacoustics Conference, Denver, Colorado*. 2017.
- [2] P. W. Cleary. "Recent advances in dem modelling of tumbling mills." *Miner. Eng.*, 14(10), 1295–1319, 2001.
- [3] P. W. Cleary and R. D. Morrison. "Prediction of 3d slurry flow within the grinding chamber and discharge from a pilot scale sag mill." *Miner. Eng.*, 39, 184–195, 2012.
- [4] J. Fischer, V. Valeau, and L. Brizzi. "Beamforming of aeroacoustic sources in the time domain." In *Inter-noise, Melbourne, Australia*. 2014.

- [5] J. Fischer, V. Valeau, and L. Brizzi. “Beamforming of aeroacoustic sources in the time domain: an investigation of the intermittency of the noise radiated by a forward-facing step.” *Journal of Sound and Vibration*, 383, 464–485, 2016.
- [6] J. Kolacz. “Measurement system of the mill charge in grinding ball mill circuits.” *Miner. Eng.*, 10(12), 1329–1338, 1997.
- [7] T. V. L. Rolf and M. Uygun. “Stress energy in ball and vibration mills.” *Bergbau*, 6, 311–318, 1982.
- [8] K. S. Liddell and M. H. Moys. “The effects of mill speed and filling on the behaviour of the load in a rotary grinding mill.” *J. South. African Inst. Min. Metall.*, 88(2), 49–57, 1988.
- [9] T. Mueller. *Aeroacoustic measurements*. Springer-Verlag, 2002.
- [10] A. Oppenheim, R. Schafer, and J. Buck. *Discrete-time signal processing*. Prentice-Hall, Inc., 1999.
- [11] Z. Prime, B. Zajamsek, and C. Doolan. “Beamforming array optimisation and phase averaged sound source mapping on a model wind turbine.” In *Internoise, Melbourne, Australia*. 2014.
- [12] I. Rakotoarisoa, J. Fischer, V. Valeau, D. Marx, C. Prax, and L. Brizzi. “Time-domain delay-and-sum beamforming for time-reversal detection of intermittent acoustic sources in flows.” *J. Acoust. Soc. Am.*, 136(5), 2675–2686, 2014.
- [13] G. Raman, R. Ramachandran, K. Srinivasan, and R. Dougherty. “Advances in experimental aeroacoustics.” *International Journal of Aeroacoustics*, 12, 579–637, 2013.
- [14] Y. Zeng and E. Forsberg. “Application of digital signal processing and multivariate data analysis to vibration signals from ball-mill grinding.” *Trans. Inst. Min. Metall. Sect. C-Mineral Process. Extr. Metall.*, 102(Jan-Apr), 39–43, 1993.
- [15] Y. Zeng and E. Forsberg. “Vibration characteristics in a large scale ball mill.” *Scand. J. Metall.*, 22(5), 280–286, 1993.